

Mars Science Laboratory Interplanetary Navigation

T. J. Martin-Mur,^{*} G. L. Kruizinga,[†] P. D. Burkhardt,[‡] F. Abilleira,[§] M. C. Wong,[¶] and J. A. Kangas^{**}
Jet Propulsion Laboratory, California Institute of Technology, Pasadena, California 91109

DOI: 10.2514/1.A32631

The Mars Science Laboratory, also called Curiosity, is a rover mission that launched on 26 November 2011 and landed on Mars 6 August 2012 in Gale Crater. The main challenges for the interplanetary navigation of the mission were to deliver the spacecraft to the correct interface point above the atmosphere of Mars and to accurately tell the spacecraft where it was as it entered the atmosphere. The spacecraft used guidance during its descent to Mars before the deployment of the parachute in order to minimize landing dispersions, resulting in a smaller landing zone that was closer to terrain of high scientific interest. This required an accurate delivery of the spacecraft to the entry interface and an update of the spacecraft state at entry, which was used to initialize the descent guidance system. Orbit determination during cruise was very accurate, being able to predict the line-of-sight position of the spacecraft after one week to within a few meters during the final weeks of approach. The spacecraft hit the top of the Martian atmosphere just 200 m from where it had been predicted to enter more than six days earlier, when it was still 2.6 million km away from Mars. This excellent level of accuracy was achieved by a combination of factors, including spacecraft characteristics, tracking data processing, dynamical modeling choices, and navigation filter setup. The accurate interplanetary navigation contributed to the very precise landing performance and to the overall success of the mission.

I. Introduction

MARS Science Laboratory (MSL), carrying the Curiosity rover, was launched on 26 November 2011 from Cape Canaveral for a 6 August 2012 landing in Gale Crater. The Curiosity rover is the heaviest vehicle ever landed on Mars [1], and it was delivered to the surface of Mars using an innovative entry, descent, and landing (EDL) system [2]. The challenge for the navigation team was to deliver the spacecraft to the right atmospheric entry interface point and to tell it where it was as it reached this point so it could safely and accurately guide itself to the proximity of the selected landing target. The landing target coordinates were chosen based on the best estimate of the performance of all the components contributing to the landing dispersion [3]. The target needed to be as close as possible to the area that the scientists wanted to explore while at the same time ensuring that the vehicle would successfully land with a high confidence level. Descent, landing, and surface-mobility hazards had to be assessed around the proposed landing zone, and a number of landing targets were evaluated using the criteria previously outlined.

One of the innovations of MSL with respect to previous Mars landers was the use of bank-to-steer guidance to adjust the vertical lift during the main deceleration phase of EDL. This allowed for a significant reduction in the size of the landing ellipse and prompted a change in the relationship between entry delivery errors and landing position errors. Unlike previous missions, the location of the landing

ellipse did not depend directly on where the vehicle entered the atmosphere of Mars but on how well that entry point was known by the spacecraft. Guidance allowed for a reduction in the landing ellipse from the 10-by-80 km ellipses of the Mars Exploration Rovers (MERs) [4] to just 7-by-21 km for the MSL. In a first approximation, and assuming that the atmospheric delivery was done with sufficient accuracy, the ellipse size was not affected by the offset between the nominal entry target and the actual entry point. Entry knowledge errors affected the ellipse size in two ways. First, the uncertainty of the exact entry point would contribute to the ellipse size, but since it was combined with other error contributors, such as initial attitude error and atmospheric conditions, at the expected performance levels it did not have a significant contribution to the ellipse size. Second, a known entry delivery error, if not communicated to the spacecraft, would shift the predicted ellipse by a known amount.

The challenge for the MSL navigation team was to accurately predict the trajectory of the spacecraft over the last couple of weeks leading up to entry, necessitating an intensive tracking campaign and verification of models and uncertainty assumptions. For the last 45 days, Doppler and range data were collected almost continuously, and for the last 28 days, delta differential oneway range (Δ DOR) sessions were performed twice a day, during the overlaps between the Madrid and Goldstone, and Goldstone and Canberra Deep Space Network (DSN) complexes. The forces acting on the spacecraft, gravitational and nongravitational, were assessed and accurately modeled; the latest ephemeris of Mars relative to the Earth were used; and tracking of the Mars orbiters was used to verify the level of accuracy of the MSL trajectory relative to Mars.

Presented as Paper 2013-232 at the 23rd AAS/AIAA Space Flight Mechanics Meeting, Kauai, HI, 11–14 February 2013; received 28 February 2013; revision received 10 January 2014; accepted for publication 19 January 2014; published online 8 May 2014. Copyright © 2014 by the American Institute of Aeronautics and Astronautics, Inc. The U.S. Government has a royalty-free license to exercise all rights under the copyright claimed herein for Governmental purposes. All other rights are reserved by the copyright owner. Copies of this paper may be made for personal or internal use, on condition that the copier pay the \$10.00 per-copy fee to the Copyright Clearance Center, Inc., 222 Rosewood Drive, Danvers, MA 01923; include the code 1533-6794/14 and \$10.00 in correspondence with the CCC.

^{*}MSL Navigation Team Chief, Mission Design and Navigation Section, 4800 Oak Grove Drive, Senior Member AIAA.

[†]MSL Orbit Determination Lead, Mission Design and Navigation Section, 4800 Oak Grove Drive.

[‡]MSL EDL Trajectory Lead, Guidance and Control Section, 4800 Oak Grove Drive, Senior Member AIAA.

[§]MSL Launch, Cruise, Relay, and Surface Trajectory Lead, Mission Design and Navigation Section, 4800 Oak Grove Drive.

[¶]MSL Maneuver Design Lead, Mission Design and Navigation Section, 4800 Oak Grove Drive.

^{**}MSL Maneuver Design Analyst, Mission Design and Navigation Section, 4800 Oak Grove Drive.

II. Mission Overview

The primary objective of the MSL Project was to land a sophisticated, mobile, analytical laboratory at or near a target of high scientific value on the surface of Mars in order to assess the area as a potential habitat for life: past or present [1]. MSL used an advanced EDL system that allowed for an increased landed mass over the previously used airbag or retrorocket systems, with much higher surface delivery accuracy, while minimizing landing dispersions to be able to use a smaller landing zone close to terrain of high scientific interest [2]. This required a more accurate delivery of the spacecraft to the entry interface and a late update of the spacecraft state at entry, which was used to initialize the descent guidance system.

After several down selections of the launch/arrival period, the MSL project decided on a 24-day launch period with a type 1 Earth–Mars trajectory, starting on 25 November 2011, and with a fixed arrival date of 6 August 2012 [5]. This launch/arrival combina-

tion provided dual Mars orbiter EDL relay coverage without requiring large changes in the orbital nodes of the orbiters.

In the approximately eight month time span from launch to arrival, a total of six trajectory correction maneuver (TCM) opportunities were scheduled to remove the injection bias and target to the entry aim point for the final landing site. From the many landing sites proposed by scientists, a final set of four possible sites was chosen on May of 2010, ranging in longitude from -45°E to 137°E and in latitude from 26°S to 24°N . A target within Gale Crater at about 137.42°E and 4.49°S was finally selected in July 2011. The mission design and navigation team had to provide targets to the launch vehicle provider that would allow for retargeting to any of those four landing sites. A central landing site was used to generate the targets, and analyses were performed to ensure that all sites could then be reached within the cruise propellant allocation [6].

The mission started with the cruise phase, right after the direct-to-Mars launch; followed by the approach phase, starting 45 days before entry; and ended with the EDL event. The MSL EDL system built on the heritage from Apollo, Viking, and MER, among others. The guidance algorithm used during the main deceleration phase to better target the landing site was based on the algorithm used for Apollo reentry. Lift was used by Viking to prolong deceleration, and the 21.5 m disk-gap parachute used by MSL was an extrapolation of the 16.5 m parachute used by Viking. The MSL cruise stage design was basically a scaled-up version of the one used on Mars Pathfinder and MER, whereas the transition for approach to entry was based on MER. An innovative component of the MSL landing system was the sky crane maneuver. Mars Pathfinder and MER used solid rocket motors in the backshell to reduce the terminal velocity and, in the case of MER, to minimize the lateral velocity component before impact. MSL used a descent stage separate from the backshell that lowered the rover down to the surface using tethers. This allowed for a much softer landing, removed the need for airbags, and allowed the rover to land on its own wheels.

Once the rover landed, it started the surface phase of the mission, which is planned to last at least one Martian year (687 days). The rover carries a total of 10 advanced instruments designed to assess whether Mars ever had an environment capable of supporting life. It is powered by a radioisotope thermal generator and can communicate with Earth either directly, using low and high gain X-band antennas, or through a Mars orbiting spacecraft using an uhf antenna. The rover can traverse about 40 m per day and up to a total 10 to 20 km during the primary mission, reaching up to the lower slopes of Mount Sharp.

III. MSL Spacecraft Configuration

A. Stages and Components

Figure 1 displays a breakdown of the MSL flight system, and Fig. 2 shows a detailed view of the spacecraft in its cruise configuration. The MSL flight system consisted of four major elements: cruise stage, aeroshell (heat shield and back shell), descent stage, and rover. The aeroshell enclosed the descent stage and rover. The total mass of the flight system right after separation from the launch vehicle was about 3843 kg, of which 540 kg corresponded to the cruise stage, 1333 kg for the aeroshell, 1070 kg for the descent stage, and 900 kg for the rover. The cruise stage carried about 72 kg of propellant, whereas the descent stage carried 400 kg of propellant. The aeroshell carried 145 kg of cruise balance masses and 168 kg of entry balance masses. The total mass of the entry vehicle after separating from the cruise stage and releasing the cruise balance masses was 3155 kg.

The design of the MSL cruise flight system is an extrapolation of the Mars Pathfinder and MER cruise spacecraft design, with a wider diameter and a reshaped backshell to accommodate the much larger descent stage and rover. From separation from the launch vehicle to minutes before entering the atmosphere of Mars, MSL was spin stabilized with a spin rate of about 2 rpm. The cruise stage included solar panels; the cruise propulsion system, with two propellant tanks and two thruster clusters; the heat rejection system; the attitude control system, with a star scanner and sun sensors; and the medium gain antenna for late cruise X-band communication. The antenna was oriented towards the $-Z$ axis of the spacecraft, as were the solar

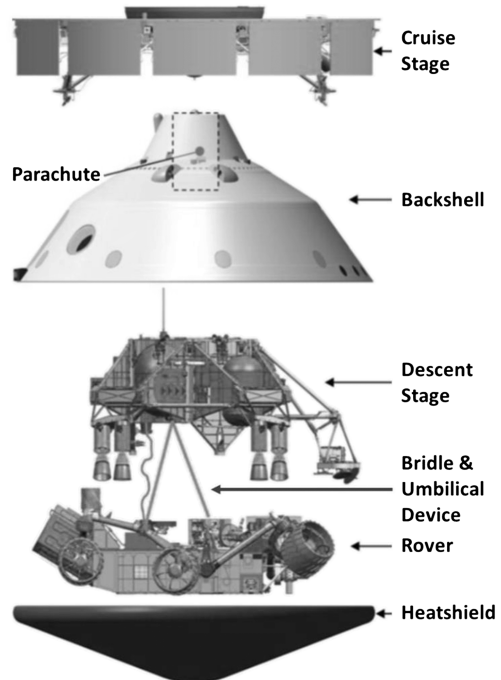


Fig. 1 Main components of the MSL flight system.

panels. The cruise stage separated from the entry stage 10 min. before entry.

The backshell, together with the heatshield, enclosed the descent stage and the rover during cruise. The parachute cone of the backshell carried not only the parachute but also two X-band low gain antennas: one in the $-Z$ direction for early cruise communication with Earth and one tilted for communication with Earth during EDL. The cone was also covered with an ultrahigh frequency wraparound antenna for communications with the relay orbiters during EDL. The backshell carried two sets of balance masses: the two cruise balance masses that, when removed, created a center of mass offset with respect to the $-Z$ axis in order to generate lift during the guided phase of EDL, and six entry balance masses that were ejected to realign the center of mass before parachute deploy. The heatshield for MSL was instrumented in order to collect engineering data during EDL and to be able to more accurately reconstruct the EDL conditions.

The descent stage carried eight reaction control thrusters, used after cruise stage separation; eight main landing engines, used after heatshield and backshell separation; and three propellant tanks that fed them. The stage also carried the inertial measurement unit (IMU) used for guided entry; the terminal descent sensor, a system with six independent radar beams used to determine the position of the spacecraft relative to the ground; a small deep space transponder

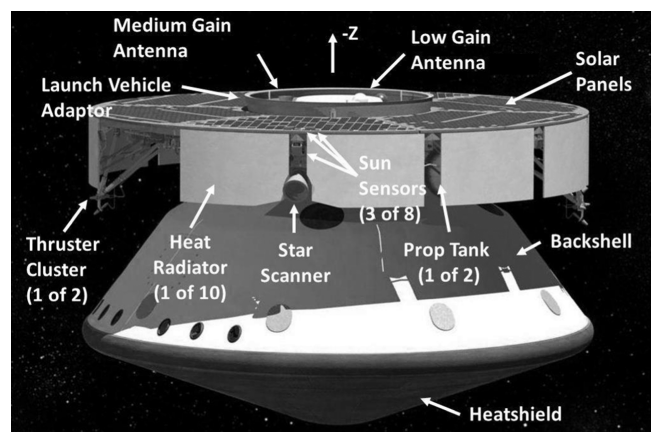


Fig. 2 MSL cruise configuration.

(SDST); and the traveling-wave tube amplifier (TWTA) used for cruise communications.

The rover was lowered from the descent stage using three bristles and an umbilical device. The rover carried another SDST and a solid-state power amplifier (SSPA), which could have been used as a backup for X-band communications during cruise. The rover carried batteries that were also used during cruise. These batteries were fully charged using the solar array days before EDL.

B. Cruise Propulsion System

The MSL cruise propulsion system was similar to that of MER: two clusters of four thrusters each in opposite sides of the solar panel, and two propellant tanks. The cruise propellant system was used to perform trajectory and attitude control maneuvers from separation from the launch vehicle upper stage to the ejection of the cruise stage. Each tank contained 36 kg of hydrazine at launch. The thrusters produced about 4.35 N of thrust each at the start of the mission, and about 3.09 N for TCM-4, the last maneuver that was executed. Each thruster cluster had four thrusters canted 40 deg with respect to the imaginary line joining both clusters. There was one thruster in each cluster canted toward $-Z$ and one toward $+Z$, whereas the other two thrusters in each cluster were canted toward each of the lateral directions. Maneuvers were performed using both clusters but could have been performed, if necessary, just using one cluster. Using both clusters allowed for balanced attitude maneuvers, and it reduced the attitude perturbation and execution error for translational maneuvers.

Four maneuver execution modes were available: two for attitude maneuvers and two for trajectory correction maneuvers. To change the direction of the spin axis, pairs of thrusters along the Z axis were fired in turns to create a torque perpendicular to the Z axis. To increase or decrease the spin rate, a matching pair of lateral thrusters would be fired to generate a torque of the appropriate sign along the Z axis. For trajectory correction maneuvers, the two available execution modes were called axial and lateral. In the axial mode, the thrusters in either the $+Z$ or $-Z$ direction would be fired simultaneously, creating a net thrust along the Z axis. In the lateral mode, the four thrusters from each cluster were fired for up to 5, out of the 30 s spin period, when they traversed the appropriate clock angle range. One of the axial thrusters in each cluster had to be fired for shorter times in order to ensure that the combined thrust vector passed through the center of mass of the spacecraft and no net torque was created. Lateral burns were more efficient in terms of propellant usage, but axial burns could be executed faster. To achieve a particular change in velocity (ΔV), the spacecraft could be rotated, and then an axial or a lateral burn could be performed at that attitude or the spacecraft could stay at its current attitude and a vector mode maneuver could be performed, i.e., combining an axial and a lateral burn.

Attitude maneuvers were performed in closed-loop mode using the sun sensor or the IMU to assess the change in attitude. When only the sun sensor was used, it was only possible to monitor the change in sun angle. Trajectory correction maneuvers were performed in open-loop mode: the total firing time would be computed on the ground and commanded to the spacecraft. Small thruster alignment errors, variations in thrust level thruster to thruster, and plume impingement effects made the attitude maneuvers not perfectly balanced in translation and created attitude disturbances and execution errors during trajectory maneuvers.

C. Cruise Telecommunications System

The MSL telecommunication system [7] can use X band for direct-to-Earth communications during all mission phases. During EDL and surface, it can also use an uhf system to communicate with the Mars orbiters. During cruise, the X-band telecommunication system was used to track the spacecraft. The system operated through one of two antennas: either a low gain antenna that was used during early cruise, or a medium gain antenna that was used during late cruise and approach. The nominal cruise telecom configuration was to use the descent stage group III SDST and the TWTA, whereas the identical rover SDST and the SSPA could be used as a backup. However, due to the lower power of the SSPA compared with the TWTA, using the

TWTA would have resulted in lower signal levels and data rates. The SDST provided the capability to transmit a signal coherent the received carrier phase, to sample the uplink ranging channel and modulate it into the downlink signal, and to modulate differential oneway ranging tones into the downlink signal.

IV. Key Navigation Requirements

The following lists the most significant high-level requirements levied on the MSL navigation function and how the requirements were fulfilled during operations.

A. Planetary Protection

1) The probability of Mars impact by the launch vehicle upper stage shall be less than 1.0×10^{-4} .

2) The probability of nonnominal impact of Mars due to failure during the cruise and approach phases shall not exceed 1.0×10^{-2} .

The launch vehicle upper stage impact requirement was fulfilled by biasing the injection aim point off the desired entry aim point to the atmosphere of Mars. The target for TCM-1 was also constrained to ensure that the second requirement was fulfilled. By the time of the TCM-2 design, it was possible to target directly to the entry point and still fulfill the requirement [8].

B. TCM ΔV and Propellant

1) The maneuver design shall ensure a 99% probability of successful targeting to the atmospheric entry point with respect to available propellant.

2) The maneuver design shall ensure that the TCM propellant budget is sufficient with 90% probability for TCM-1 delayed until launch plus 30 days.

Prelaunch maneuver analysis was performed to ensure that any of the possible landing sites could be reached for any possible launch/arrival combination using the available propellant. The very precise launch vehicle injection provided ample propellant margin. Because of concerns about the propulsion system, and to work on other early cruise issues, TCM-1 was postponed from its prelaunch location, which was set to be launch plus 15 days. A lateral calibration maneuver was executed on December 22 (launch plus 26 days) and TCM-1 on January 11 (launch plus 46 days). During cruise, 21.2 kg of propellant were used for the TCMs, and 7.3 kg was used for attitude maneuvers, with 43.5 kg of cruise propellant left in the tanks at the time of cruise stage separation.

C. Atmospheric Entry Delivery and Knowledge Accuracy

1) The entry vehicle shall be delivered to the specified atmospheric entry conditions with an inertial entry flight-path angle error of less than or equal to 0.20 deg.

2) The EDL guidance system shall be initialized with an entry state with an accuracy of 2.8 km in position and 2.0 m/s in velocity.

3) The navigation system shall support performing the final update of the entry state vector not later than entry minus 2 h.

Based on a postlanding cruise trajectory estimation using all the data and calibrations up to entry, the actual EFPA was 0.013 deg shallower than the -15.5 deg target, and the onboard entry state was just 200 m in position and 0.11 m/s in velocity off from the postlanding reconstructed entry state. That final onboard entry state was calculated and uploaded to the spacecraft six days before entry, and no further updates were found to be necessary.

V. MSL Navigation System

The MSL navigation system was composed of three major parts: trajectory modeling and determination, trajectory control maneuver design and analysis, and EDL and relay trajectory analysis. Navigation functions during cruise included the following:

1) Estimate the spacecraft trajectory based on radiometric tracking data: Doppler, range, and delta differential oneway range measurements.

- 2) Generate spacecraft ephemerides and ancillary trajectory data products for the DSN and the mission operations teams.
- 3) Perform EDL trajectory analysis to determine the desired atmospheric entry aim point and to evaluate landing dispersions.
- 4) Determine the desired ΔV vector for TCMs and verify the maneuver implementation generated by the spacecraft team.
- 5) Provide real-time tracking data residual monitoring during TCMs, EDL, and other dynamic events.
- 6) Reconstruct TCM ΔV using pre- and post-TCM tracking data.
- 7) Perform EDL trajectory analysis to provide inputs for uplink of EDL parameter updates.

The remainder of this section describes the data, models, and processes used for navigation analysis.

A. Tracking Data Types

The tracking data types that were used for MSL orbit determination were two-way coherent Doppler, two-way coherent sequential range, and Δ DOR [9]. MSL did not have an oscillator stable enough to provide usable one-way Doppler data. The data were collected by the 34 and 70 m antennas of the Deep Space Network at Canberra, Australia; Goldstone, California; and Madrid, Spain. Doppler data provided a high-resolution high-accuracy measurement of the line-of-sight velocity of the spacecraft with respect to the ground antennas, at a noise level of about 0.1 mm/s for 300 s compression time. Range provided an accurate measurement of the line-of-sight distance to the spacecraft, with an accuracy of about 1 m. Δ DOR provided a measurement of the plane-of-sky angle error with respect to nearby quasars, with accuracies at the 1.5 nrad level (40 ps differential range) for one session, or around 400 m at the Mars arrival distance during final approach. This combination of data types resulted in typical position error covariance ellipsoids that looked like a pancake: very narrow in the line-of-sight direction and wider in the plane-of-sky directions. Increased bandwidth between the Jet Propulsion Laboratory, California Institute of Technology (JPL) and the DSN complexes allowed for fast delivery of Δ DOR data, with a total possible turnaround time from collection to delivery to the navigation team of less than 3 h when personnel were on site.

Like other previous Mars missions, excluding the Mars Reconnaissance Orbiter (MRO) approach optical navigation experiment, MSL flew to Mars using data collected at Earth. MSL did not have any means to track Mars, either optically or radiometrically, before arriving at its atmosphere.

For some of the MSL Goldstone–Canberra Δ DOR sessions (once a week for the final two months before Mars arrival), data from the Mars Odyssey and Mars Reconnaissance Orbiter were also collected. Δ DORs were generated for the orbiters and for MSL: double-differenced carrier phase measurements, of increased resolution, were created between MSL and the orbiters. The MSL navigation team processed range and Δ DOR data for the Mars Odyssey and the Mars Reconnaissance Orbiter using the reconstructed Mars-relative trajectories provided by their respective navigation teams and the latest Mars ephemeris in order to assess how well the Mars ephemeris was predicting the position of Mars. The double-differenced phase measurements were similarly processed to assess the plane of sky error of MSL relative to Mars.

The Deep Space Network provided media, troposphere and ionosphere, and Earth orientation calibrations that were used when processing the tracking data.

B. DSN Tracking Schedule

The DSN tracking schedule used for prelaunch navigation analysis is listed in Table 1. The number of tracking passes during early and midcruise was not driven by navigation requirements but driven instead by operational considerations. To accommodate spacecraft checkout activities and software uploads during operations, the number of passes was actually higher. Overall, the DSN performance was excellent. A total of 79 Δ DOR sessions, counting both the Goldstone–Madrid and the Goldstone–Canberra baselines, was successfully executed, including 10 multispacecraft collections. Two of the Δ DOR sessions were not successful due to tracking equipment

Table 1 MSL tracking schedule

Start	End	Doppler/range passes	Δ DOR sessions
Launch	L + 30d	Continuous	None
L + 30d	E – 67d	Five per week	One per week
E – 67d	E – 45d		Two per week
E – 45d	E – 28d	Continuous	
E – 28d	Entry		Two per day

problems. The effect of this was most noticeable when only one Δ DOR session per week was being performed. Losing that session meant not having data from one of the baselines for almost a month.

C. Trajectory Modeling

A key contributor to good navigation performance is being able to accurately predict the trajectory of the spacecraft relative to its target. The ephemeris of Mars is periodically updated using the latest range and Δ DOR measurements to the Mars orbiters. MSL used two releases of the planetary ephemeris during operations: DE424, generated two months before launch [10]; and DE425, generated three months before arrival. The update in the position of Mars at the time of MSL arrival between these two ephemerides was small, just tens of meters. The actual error of the ephemeris was probably not more than 100 or 200 m, as demonstrated by the dual spacecraft tracking, which was at the error level of the Δ DOR data used to generate them.

A spacecraft trajectory is affected by gravitational and non-gravitational forces. The gravitational forces are known with high accuracy, consistent with the accuracy of the planetary ephemerides. The main nongravitational forces acting on MSL during cruise were outgassing during the first two weeks after launch, solar and thermal radiation pressure, thrusting for trajectory correction maneuvers, and the effect of the slight unbalance of the thruster pairs during attitude maneuvers. A prelaunch solar and thermal radiation pressure model was constructed using spacecraft dimensions, surface properties, and data from the thermal team. This model was then fit using a truncated Fourier series expansion in terms of sun colatitude in order to generate a simpler parameterization of the combined effect. Experience with previous missions showed that estimating surface reflectivity parameters sometimes produced nonphysical values, e.g., negative values. The new model was tested using MER data and allowed for a similar fit using a much smaller number of parameters.

TCMs were calibrated using tracking data, and the results of these calibrations were provided to the propulsion and attitude control system (ACS) teams so they could better predict thruster performance in future maneuvers. The residual translational ΔV from attitude turns was assessed during the ACS/navigation (NAV) calibration by using a series of especially designed turns that allowed observing all components of the resulting ΔV .

D. Orbit Determination

The orbit determination filter performed a weighted least-squares minimization of the tracking data residuals and the a priori parameter constraints. Two key considerations in the MSL orbit determination strategy [11] were to accurately assess the uncertainty of the parameters that were either being estimated and constrained, or being considered, and to properly weight the tracking data, so that the final fit would be consistent with the expected accuracy of the data and the covariance estimates would be accurate.

To realize the highest possible accuracy in the Doppler data, and since MSL was a spin-stabilized spacecraft, the spin effects on the data had to be accurately modeled and removed [12]. Since the X-band signals used by MSL were circularly polarized, the spinning of the spacecraft introduced a bias in the Doppler proportional to the spin rate. In addition, since the spacecraft antennas were not located along the spin axis, a signal with the same period as the spin period was being added to the center-of-mass Doppler. The MSL navigation team used the antenna coordinates with respect to the center of mass and the periodic Doppler signature to estimate the rotational state of

the spacecraft. Then, the estimated rotational state was used to calculate and remove the periodic signature and the bias from Doppler and range. The end result produced measurements relative to the center of mass. This process was performed using small Doppler compression times: 1 to 5 s. After the data were corrected, the Doppler measurements were compressed to 300 s for use by the orbit determination filter. The data were accurate enough that the antenna phase center change with clock angle was observable. Also, using several passes of data, it was possible to estimate the full attitude and the antenna arm with respect to the spin axis.

The MSL filter configuration allowed for the estimation of interplanetary medium charged particle delays. During early cruise, solar coronal mass ejections produced significant biases and an increase in the noise of the tracking data. However, postlanding reanalysis of the data showed that the effect of these delays could have been neglected with a very small impact on the quality of the resulting trajectories. The charged particle delay estimates reduced the measurement residuals but did not significantly move the solution.

A number of data arc lengths were used during operations, with the start of the data arc advanced in order to remove earlier data and reduce the amount of time required to generate an acceptable orbit determination solution. For some of the orbit determination data cutoffs and arcs, several filter configuration strategies were evaluated to assess what the effect of changing the baseline assumptions was on the estimated solution and its covariance [13].

E. Trajectory Control

The targets provided to the launch vehicle for MSL injection into an Earth-to-Mars trajectory did not directly aim for the Gale crater atmospheric entry point. The aim point was moved away from Mars so that the probability of the launch vehicle upper stage hitting Mars was low, and the time of closest approach (TCA) was selected so the highest cost of retargeting to any of the downselected landing sites was minimized.

Table 2 shows the prelaunch maneuver plan and the actual dates for the TCMs executed during operations, shown also relative to either launch (L) or entry (E) [8]. TCM-1 and TCM-2 were optimized jointly in order to minimize total propellant and to fulfill planetary protection requirements. TCM-2 was reoptimized after TCM-1 was executed in order to correct for TCM-1 delivery errors and to directly target the atmospheric entry target. According to prelaunch analysis, which used conservative maneuver execution error assumptions, TCM-5 should have been the last maneuver needed to fulfill the delivery requirements. Good trajectory prediction and maneuver execution performance allowed for TCM-5 to be cancelled. TCM-6 was a contingency opportunity available to correct unexpected gross delivery errors that may have compromised the capability of the EDL system; it was also not needed and was canceled.

The orbit determination data cutoff (DCO) was seven days before the maneuver execution time for TCM-1, TCM-2, and TCM-3; 13 h for TCM-4 and TCM-5; and 5 h for TCM-6. The placement of TCM-6 in the timeline was a compromise between the need to observe the trajectory error before the TCM DCO, as the spacecraft was pulled by Mars, and the ability to reconstruct the trajectory after the maneuver, in order to accurately initialize the EDL guidance system.

TCM design was performed using an open-loop simulation of the EDL trajectory. It was targeted to the landing site but moved north by

8 km at the entry point in order to avoid recontact of the cruise stage with the entry stage.

The decisions to execute or not to execute TCM-5 and TCM-6 were based on crosstrack and entry flight-path angle thresholds [14]. For TCM-5, the thresholds were set such that the delivery envelope was within the spread of the many EDL Monte Carlo simulations that were performed during development. For TCM-6, the thresholds were wider and were set to ensure that the EDL system would have enough margins to land successfully.

Since the launch vehicle injection was very accurate and, consequently, the cruise propellant margin was ample, all TCMs were executed at the current cruise attitude and pre-TCM turns were not necessary. TCM-1, TCM-2, and TCM-3 were executed in a no-turn vector mode, with axial and lateral burns executed in sequence, whereas TCM-4 was executed with just a lateral burn. TCM power and telecommunication constraints, while evaluated during TCM design, never played a role in determining the type of maneuver implementation.

F. Entry, Descent, and Landing Analysis

The navigation team collaborated with the EDL engineering team in order to perform EDL simulations; analyze EDL performance; and evaluate changes in the EDL system, its configuration, and its initialization [15]. The orbit determination team generated entry state files, containing typically 8001 delivery and knowledge states, which were then used to perform EDL Monte Carlo simulations. One of the results of each Monte Carlo was the landing points file, which listed the achieved landing point for every knowledge/delivery pair of states. This file was processed together with a landing hazards file in order to arrive at an estimate of the landing success probability.

As discussed previously, one very significant difference between MSL and previous Mars lander missions was the fact that MSL used entry guidance. For previous missions, the landing point location was directly correlated with the point at which the spacecraft entered the atmosphere of Mars. That was not the case for MSL. The vehicle was told at what point it was entering the Martian atmosphere and what the landing target was. It could then guide itself to the landing target using bank angle modulation during its preparachute hypersonic flight. This meant that, as long as the delivery was done within the range of entry conditions that the guidance could compensate for, and assuming perfect knowledge, the center of the landing ellipse was not significantly affected by the actual entry point. That is why TCM decisions were based on entry flight-path angle and crosstrack thresholds, and they were not based on the location of the landing ellipse with and without a TCM. In addition, the size of the delivery ellipse was dominated by factors not controlled by navigation, such as atmospheric density fluctuations, winds, attitude initialization, and EDL system guidance performance. The effect of the expected trajectory knowledge errors was much smaller than some of those other factors listed. Errors in the predicted entry state sent to the spacecraft would directly map to the ground but, again, those were expected to be small and did not affect significantly the overall landing success rate. The difference between the state currently in the spacecraft and the latest available predict was evaluated during the entry parameter update opportunities. The differences were always found to be small when compared with the expected uncertainty of the estimate, and they did not make a significant difference on the ground.

Table 2 TCM schedule

TCM	Prelaunch planned date	Actual execution date	Description
Lateral Calibration	Not planned	December 22, L + 26d	Test of the cruise propulsion system
TCM-1	L + 15 days	January 11, L + 46d	Remove injection bias and error, target to the selected landing site.
TCM-2	L + 120 days	March 26, L + 121d	Correct TCM-2 delivery errors
TCM-3	E - 60 days	June 26, E - 40d	Correct TCM-3 delivery errors
TCM-4	E - 8 days	July 28, E - 8d	Correct TCM-4 delivery errors
TCM-5	E - 2 days	Waived off	Backup TCM-5 opportunity
TCM-5X	E - 1 days	Not needed	
TCM-6	E - 9 h	Waived off	Contingency opportunity to correct nonsurvivable delivery errors

G. Orbiter Relay Support

The navigation team produced EDL relay targets that were used by the currently operational Mars orbiters, NASA's Mars Odyssey and Mars Reconnaissance Orbiter, and ESA's Mars Express to design orbit change strategies that would ensure that the orbiters would be able to receive the uhf signal from MSL during EDL [16]. It was not necessary to request that the orbiters change their orbital planes, but the location within the orbit needed to be changed so each of the orbiters would be in a favorable geometry to provide coverage of the EDL event. The targets were adjusted as the location and time of MSL entry were refined, and the telecommunications performance was evaluated to assess whether additional changes to the orbiter trajectories were warranted. The team also generated surface trajectory predicts and products to assist with surface mission planning, and it continues to do so during the surface phase of the mission.

VI. Navigation Results

A. Launch and First Station Acquisition

Before launch, the project planned and tested a strategy to deorbit the spacecraft for the hypothetical case in which the launch vehicle was not able to escape Earth's orbit. To minimize the probability of the nuclear fuel pellets rupturing, it was planned to deorbit the spacecraft using the descent stage reaction control system thrusters over a depopulated area of the Pacific Ocean. Fortunately, this was not needed for MSL, but the orbit determination and trajectory modeling processes and tools prepared for this contingency were used to support the unsuccessful Fobos–Grunt recovery effort.

MSL was very accurately launched in an Atlas V 541 from the Cape Canaveral Air Force Station Space Launch Complex 41 on 26 November 2011, at 15:02:00 Coordinated Universal Time (UTC), on the first launch opportunity of the second day of its launch period; the launch had to be delayed by one day to replace one of the flight termination batteries of the launch vehicle. The navigation team prepared spacecraft mode transition commands for every launch opportunity of every launch day of the launch period. As the launch and separation times changed from opportunity to opportunity, the mode timers needed to change to ensure that the spacecraft was in the proper configuration to enable prompt initial station acquisition after separation.

Initial acquisition by the Deep Space Network station in Canberra occurred at 15:52:29 UTC. Since the spacecraft was so close to the station, the signal was stronger than what could be received by the 34 m antennas and the stations were configured to receive at the opposite polarization to reduce the received signal level. This unfortunately allowed reflected multipath to mix with the directly received signal and greatly increased the Doppler noise. In addition, the angle measuring system at Deep Space Station 34 (DSS-34), equipped with an acquisition aid antenna, did not work properly and did not produce usable angle measurements. Despite all this, and helped by the excellent injection performance, the navigation team was able to prepare pointing predicts for subsequent passes, for which the proper signal polarization was used, and acquisition and tracking afterward were nominal. The calculated injection error was 0.23 sigma of the pre-launch injection accuracy estimate [17]. That meant that the cost to correct the injection error was small when combined with the removal of the injection bias and the landing site retargeting. Preliminary EDL relay targets were sent to the orbiter teams within a week after launch so they could start phasing their trajectories for EDL relay coverage.

B. Early Cruise

The injection was so accurate that the execution of the first TCM could be postponed. This allowed the cruise team to have time to investigate unexpected issues with the spacecraft computer; the anomaly was discovered the first time the star scanner was used and forced the star scanner to be switched off until the issue was resolved. Navigation provided the attitude control team with Earth angle estimates based on the Doppler spin signature, and these values were combined with the sun sensor data to produce spacecraft attitude estimates in absence of star scanner data [12]. These estimates were used for the early spacecraft turns, required to maintain adequate power and telecommunications performance.

Outgassing accelerations were evident during the first two weeks of cruise, and small stochastic accelerations had to be estimated in order to get a good fit of the tracking data [11]. By mid-December, the level of the outgassing acceleration was small enough that it could be neglected.

Due to concerns about the propellant valves, the project decided to perform a lateral calibration maneuver before TCM-1 in order to assess the health of the cruise propulsion system. The maneuver, which was composed of two lateral burn segments with a combined ΔV of 0.555 m/s, was executed on 22 December 2011, resulting in an underburn of just 1.7% with a misspointing of less than 0.5 deg; a very good performance considering that this was MSL's first translational maneuver. TCM-1 was then executed on 11 January 2012, with an axial burn of 1.585 m/s and a lateral burn of 5.611 m/s. TCM-1 was designed to reduce the B-plane miss distance from 47,513 to 4956 km and the TCA from 14 h 50 min. to 34 min. The B plane is a planet-relative coordinate system that is frequently used for targeting encounters and flybys [18]. The B plane is perpendicular to the arrival V infinity, and its two coordinates are named $B \cdot R$, along the South Pole direction, and $B \cdot T$, contained in the equatorial plane. The total TCM-1 maneuver execution error was small at only $+2.3\%$ in magnitude and 0.52 deg in pointing. Both the lateral calibration maneuver and TCM-1 were executed using ground calculated attitudes based on Doppler and sun sensor data.

On 25 January 2012, an ACS/navigation calibration was performed in order to assess the residual translational ΔV resulting from spacecraft turns. The activity consisted first of a turn away from the Earth line to an Earth angle of about 40 deg, and then of two sets of four turns, each set consisting of turns of about 4.5 deg away and toward the Earth line and then around the Earth line and back. The estimated translational ΔV from the calibration was small, less than 0.03 mm/s per degree, with a repeatability of about 0.002 mm/s per degree, or about 0.02 mm/s for a typical late-cruise turn. These estimates were used to calculate the a priori ΔV values for future turns, and corrections to those ΔV were estimated with a constraint of 0.005 mm/s per degree.

Toward the end of January, the sun started to be more active, and on January 27, an X-class coronal mass ejection was unleashed in the Earth's direction. The effect on the range and Doppler residuals of the increased density of charged particles between the Earth and MSL was clearly observable, and the orbit determination filter was changed in order to estimate charged particle delays, so that these effects would not adversely affect the trajectory estimate.

C. Midcruise

Post-TCM-1 orbit determination was fairly stable. On 28 February 2012, the spacecraft was commanded to switch from using the low gain antenna to use the medium gain antenna, resulting in an observed decrease in tracking data noise, both due to increased received power and reduced antenna pattern effects [12].

As the distance to the sun changed rapidly, so did the angle between the spin axis and the sun direction (Fig. 3). It was obvious that the ΔDOR fit was getting worse and that turn ΔV estimates were not consistent with the ACS/NAV calibration values. Early in cruise, a solar radiation pressure model with a total of 12 parameters was used. This model provided a very good fit of the prelaunch solar and thermal acceleration calculations, and it was able to fit MER data very well for its whole cruise. One of the differences between the MER and MSL missions was that MSL was equipped with a multi-mission radioisotope thermal generator (MMRTG), which produced heat and electricity for the rover. The thermal output of the generator was about 2 kW, which was equivalent to 5–10% of the solar power received by the spacecraft. That energy was dissipated during cruise, mostly through the radiators of the heat rejection system, but part of it was also being radiated through the backshell. Since the acceleration due to solar radiation pressure was being scaled with the inverse of the square of the distance to the sun, the contribution of the MMRTG was not being properly modeled by being part of the solar radiation pressure model. The solar and thermal model was changed to have just three bias parameters for solar effects, one per axis, and a weekly

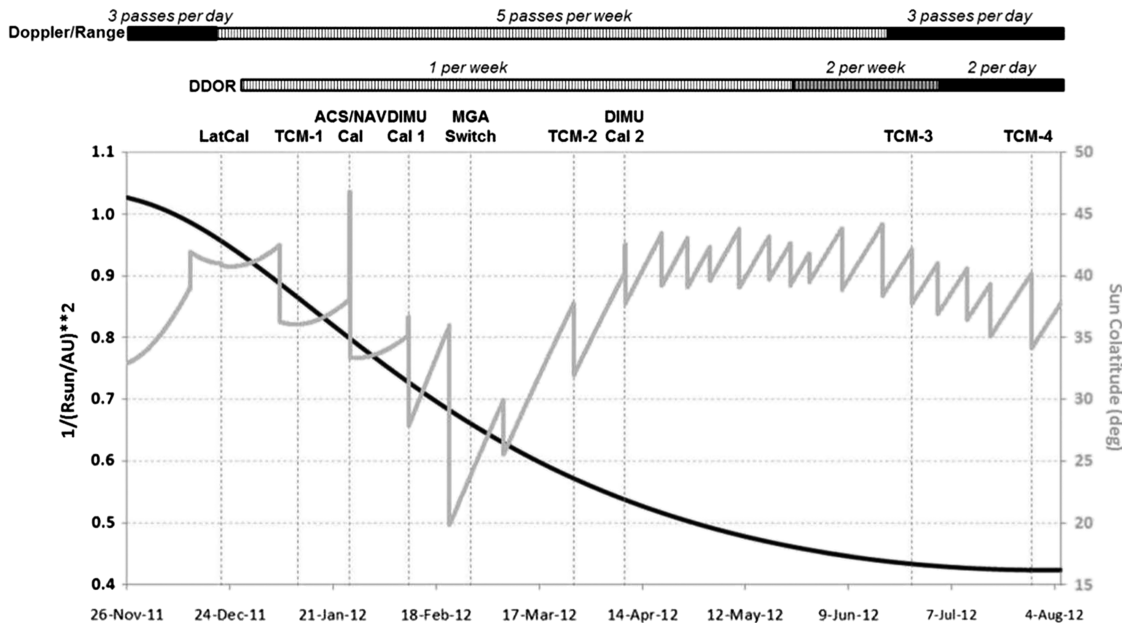


Fig. 3 Tracking plan, inverse of the square of the distance to the sun, and sun colatitude as a function of time.

stochastic acceleration along the Z axis of the spacecraft to fit changes due to solar panel utilization, component temperature, and MMRTG heat radiation. After this update, the Δ DOR fit was as expected, turn ΔV estimates stayed at their predicted levels, and future data passthroughs improved significantly.

Prelaunch planning had assumed a combined TCM-1, TCM-2, and TCM-3 optimization to reduce the probability of nonnominal impact with Mars. Once TCM-1 was executed, it was not necessary anymore to bias TCM-2 away from the entry target, so TCM-2 was aimed directly to the Gale atmospheric entry interface point. TCM-2 was executed on 26 March 2012. It consisted of an axial burn of 0.195 m/s followed by a lateral burn of 0.726 m/s, with a resultant total B-plane change of 5002 km, and the TCA shifted later by 21 min. and 30 s. The maneuver was executed with almost zero magnitude error and a 0.4 deg pointing error.

Soon after TCM-2 execution, mission management requested to delay TCM-3 in order to load and upgrade the flight software and to perform instrument checkouts. There was no negative impact of such a delay, so TCM-3 was postponed 19 days, and it took place on 26 June 2012.

During midcruise, two calibrations of the descent stage inertial measurement units (DIMUs) were performed. The EDL guidance system used the DIMU data to find its way to the landing site, so these calibrations were important for estimating biases in the measured acceleration and turn angle. The DIMU calibrations consisted of sets of fairly big turns. After the second calibration was completed, it was noticed that the observed turn ΔV were significantly smaller than the values predicted during the ACS/NAV calibration. Subsequent turns exhibited a similar trend, with decreasing line-of-sight Doppler offsets. Ultimately, it was decided to estimate an overall turn ΔV scale factor as a weekly stochastic and increase the turn ΔV uncertainty by a factor of two.

In May 2012, the solar system dynamics group released the final planetary ephemerides update for MSL: DE425. The changes with respect to the ephemerides previously used, DE424, were small: about 25 m at the time of MSL arrival to Mars. The navigation team incorporated the update and started using the Earth–Mars covariance recommended for the new set. The covariance corresponded to a predicted arrival uncertainty of about 100 m in right ascension, 150 m in declination, and 10 m in range.

D. Late Cruise

The successful use of the entry state by the entry guidance algorithm to find its way to the landing site relied not only on the accuracy of the state but also on the accuracy of the spacecraft timing system.

An error of 1 s when timing the initial state would map into an error of about 6 km in position. While the correlation of onboard time with ground time is something that has been done successfully in many missions by transmitting timing packets, it was desired to verify that this correlation was being done properly for MSL. The method that was used was to compare the attitude state estimates (in particular, the clock angle) between the onboard attitude estimate that used the sun sensor and the method used to remove the Doppler signature. High-rate ACS telemetry was collected over a period of almost 8 h, and it was then used to generate a time-tagged attitude file. This attitude file, with different offsets in the time tags, was used by navigation to model the spin signature. The time offset that produced the smallest residuals was just about -0.015 s, well within the timing accuracy needed for a safe landing.

The successful execution and analysis of calibrations and verification activities during cruise allowed for a reconsideration of the size of the landing ellipse. Prelaunch planning had used an ellipse size of 20 by 25 km, but Monte Carlo simulations using the latest assumptions during later cruise produced an ellipse size of 7 by 21 km. Since Curiosity could not safely land at the rugged area in the slopes of Mount Sharp that would be its final scientific destination, it was expected to drive there from a nearby, safer landing location. Therefore, there was an opportunity to reduce the length and duration of the surface drive by moving the landing target closer to the area preferred by the science team. Different landing targets were evaluated, and the final landing target coordinates were selected by choosing a point as close as possible to the science area that did not significantly decrease the total probability of success integrated over the landing ellipse. This was done for a number of plausible ellipse sizes based on optimistic, baseline, and conservative assumptions. The resulting landing target was about 6.5 km south and 1.3 km west from the original landing target. The adjustment in the landing target changed the B-plane and TCA targets, and it was those new targets that were used for the final TCM-3 design.

TCM-3 was executed on 26 June 2012, as a no-turn vector-mode maneuver with an axial burn of 27.7 mm/s and a lateral burn of 25.6 mm/s. One week later, after two Δ DOR sessions were collected for each DSN baseline, the execution estimate had a magnitude error of 1.1%, and a pointing error of 2.4 deg. The error, while within the requirements, was proportionally higher than for previous maneuvers for two reasons: it was a much smaller maneuver and it required a +Z axial burn, whereas TCM-1 and TCM-2 had used -Z axial burns. The consequence was that the resulting entry flight-path angle was predicted to be outside of the 0.2 deg corridor, and a TCM-4 would be needed to correct this.

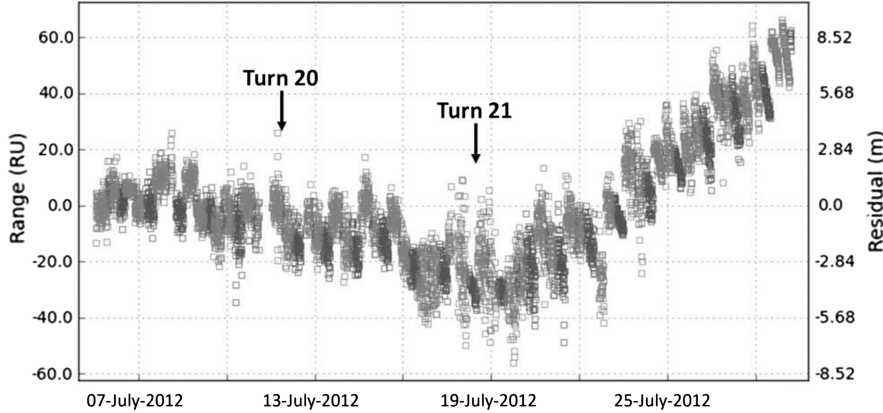


Fig. 4 Range passthrough residuals up to TCM-4. One range unit (RU) is about 28 cm.

Orbit determination following TCM-3 was very stable, with the line-of-sight residual passthrough for the aforementioned solution being within ± 10 m after three weeks of prediction (Fig. 4). The period between TCM-3 and TCM-4 was similar in sun–spacecraft distance and solar angle to the period between TCM-4 and entry, so this period was used to refine the solar and thermal radiation pressure model that would be used for the final approach.

Δ DOR and range data for the orbiters continued to be processed to confirm the accuracy of the Mars ephemeris, and spacecraft-to-spacecraft phase very long baseline interferometry (VLBI) measurements were taken and processed to assess the quality of the MSL trajectory with respect to Mars (Figs. 5–7).

Two weeks before Mars arrival, and in preparation for TCM-4 design, the navigation team started to receive and use daily media and Earth orientation parameter calibrations.

E. Final Approach

TCM-4 was executed on 28 July 2012, as an 11 mm/s lateral-only maneuver, and it was immediately followed by the last turn before arrival to Mars. The lateral-only maneuver mode could not fully correct for entry time or entry flight-path angle, but it resulted in just one-third of the size of the vector-mode implementation. This lateral-only maneuver mode was assumed to be more accurate than the vector mode, and the expected entry time and flight-path angle misses were not large enough to be of concern. The line-of-sight Doppler error during the maneuver was +4.6%.

Thirty-five hours after TCM-4 was executed, 6.5 days before entry, and after just one Δ DOR session from each DSN baseline, an orbit determination solution was obtained to calculate the first entry state that would be uploaded into the spacecraft, called entry parameter update 1 (EPU1). There were three additional opportunities to update the entry state and two additional opportunities to execute another maneuver if required. To validate the final attitude estimate obtained by the ACS team, several days after TCM-4, the navigation team

generated a Doppler-based attitude solution using data from multiple passes after that maneuver and obtained an attitude solution that was 0.023 deg from the attitude calculated by ACS using star scanner data, well within the requirements for attitude initialization before EDL.

At the TCM-5 decision point, the orbit determination solution was still well within the decision box, so the maneuver implementation for TCM-5 was cancelled. When the entry parameter updates for the data cutoffs at entry minus 33, 14, and 6 h were evaluated, the orbit solutions had not moved significantly, either in the B plane (Fig. 8) or when propagated to the ground using EPU1. Therefore, all further scheduled updates of the onboard state were cancelled. By the time of the last update opportunity, the line-of-sight residuals with respect to the EPU1 solution were just 2 m off from the predicted values. TCM-6 was also waved off. After processing all of the two-way data before entry, the latest estimate of the entry state was just 200 m away from

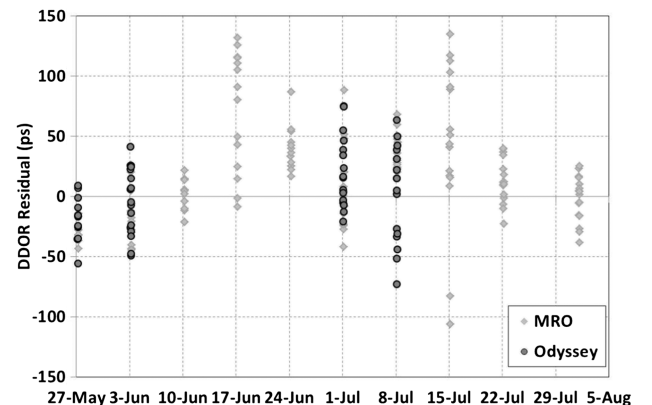


Fig. 6 Orbiter Δ DOR residual with DE425.

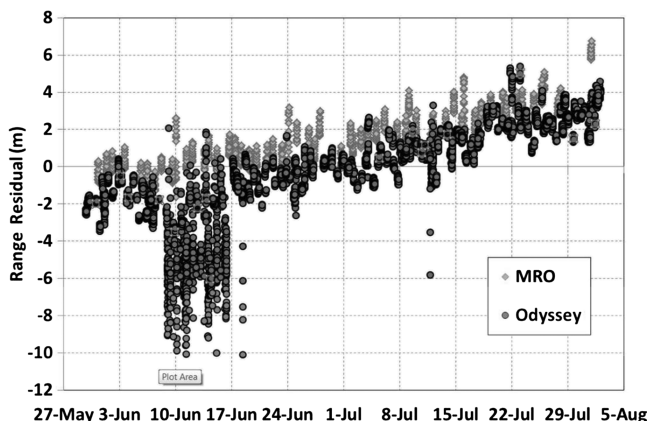


Fig. 5 Orbiter range residuals with DE425.

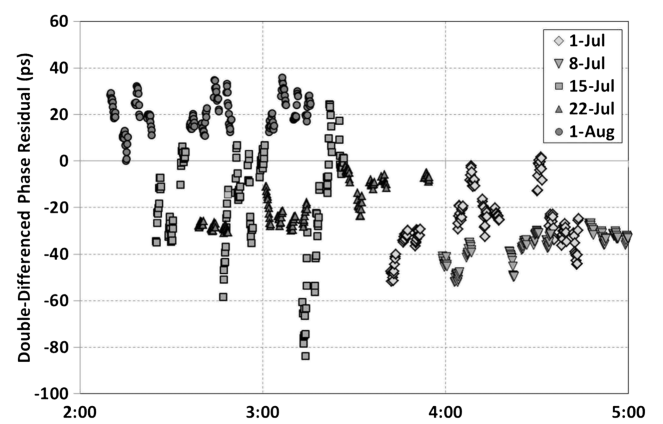


Fig. 7 MSL–MRO double-differenced phase VLBI residuals.

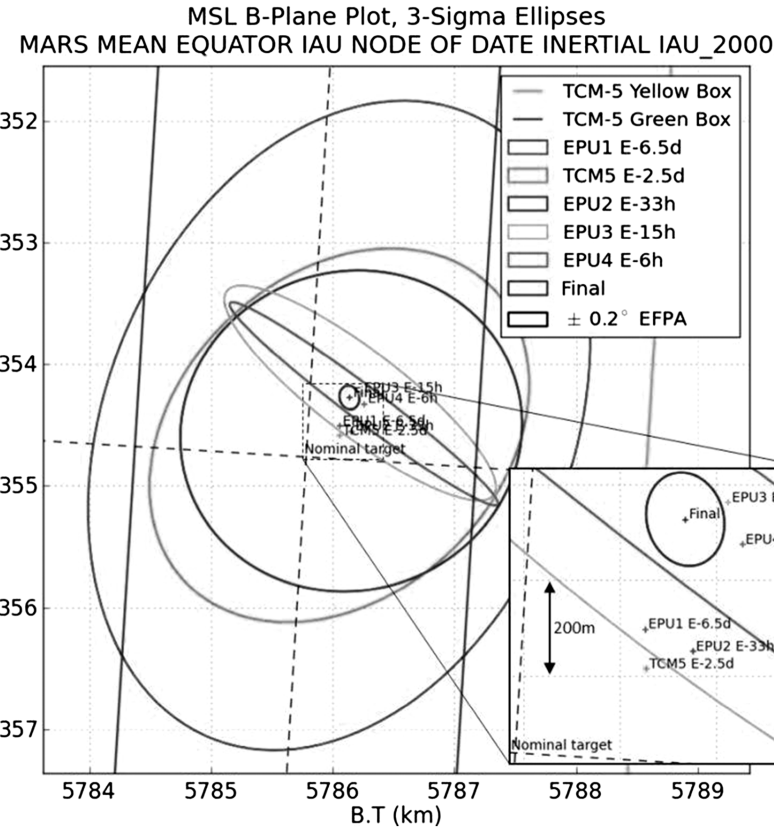


Fig. 8 Three-sigma B-plane error ellipses in the conventional International Astronomical Union (IAU) Mars reference frame for TCM-5 and EPU DCOs.

the EPU1 state. During these last days, the trajectory prediction was so stable that the solution sometimes moved away from the earlier prediction when ΔDORs without updated media calibrations were added, only to move back when the corresponding calibrations were received (Figs. 9 and 10).

Oneway Doppler data were used to confirm atmospheric entry and parachute deployment, but this link was lost approximately 5 min. after entry, a few seconds before the spacecraft was occulted behind Mars as it descended on its parachute. Real-time uhf telemetry relayed by Odyssey confirmed a successful landing, with the first images from the hazard detection cameras being received just minutes after touchdown.

F. Rover Position Determination

MRO imaged MSL while decelerating on the parachute, and the MSL Mars Descent Imager (MARDI) took photographs of the surface as it descended, allowing for a prompt determination of the actual landing site. Curiosity landed about 2.4 km east and 400 m north of the target. As soon as two-way DSN Doppler data were collected, the navigation team also produced radiometric estimates of the rover position. The final radiometric estimate, using all the coherent DSN data collected before the rover started moving, was 76 m north from the MARDI estimate, with a one-sigma latitude uncertainty of 62 m. The radiometric solution would have benefited from two-way uhf Doppler between the rover and the orbiters, but

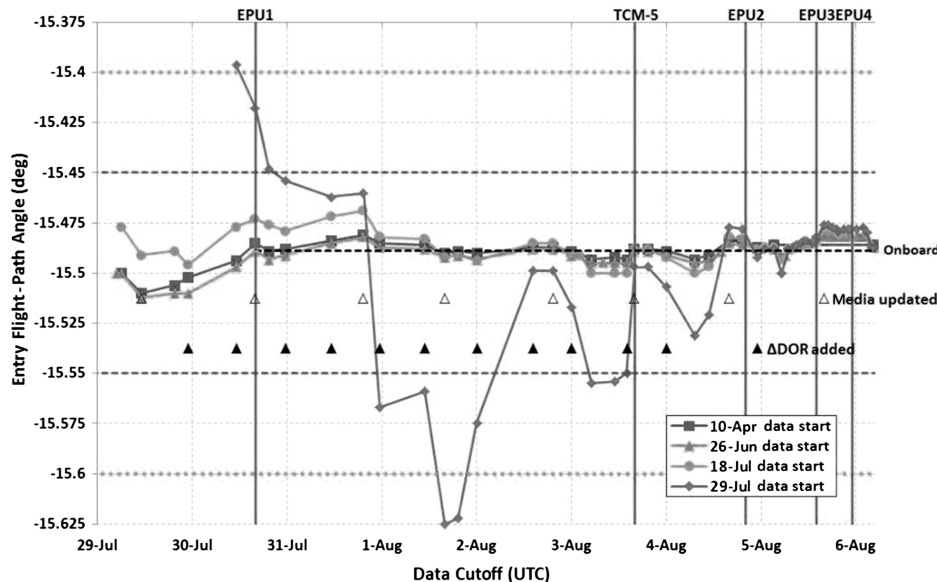


Fig. 9 Entry flight-path angle evolution after TCM-4.

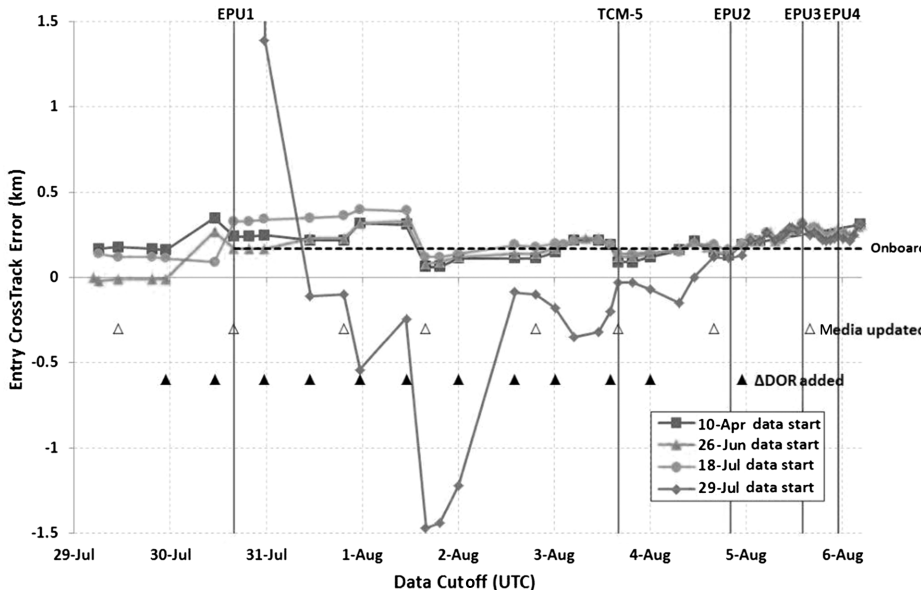


Fig. 10 Entry crosstrack error evolution after TCM-4.

since the location was already well determined with MARDI data, no uhf Doppler data were collected.

VII. Postlanding Assessment of the Interplanetary Navigation Performance

Prelaunch analysis had been performed to verify that the previously stated requirements could be fulfilled for any of the possible landing sites and launch-arrival periods that were being considered by the project [19]. For this analysis, two sets of results were computed: one using the stated requirements and conservative performance assumptions for the factors affecting the navigation function, referred to as baseline; and another using the best estimate of what those factors would be during operations, referred to as no margin. For example, the cruise propulsion system had stated requirements of what the TCM execution accuracy should be, but it used the same components as those used by MER. The baseline analysis used those stated TCM requirements in order to assess the TCM execution accuracy, whereas the no-margin analysis used values based on the actual performance seen for the MER spacecraft.

The baseline results were used to plan the schedule of TCM and parameter update opportunities, since there was no guarantee that the very good performance seen in the MER spacecraft and other previous missions would be repeated. The plan for the final approach was to have trajectory correction maneuver opportunities at entry minus eight days (TCM-4), entry minus two days (TCM-5), and entry minus 9 h (TCM-6); and entry parameter upload opportunities with data cutoffs at entry minus 6.5 days (EPU1), entry minus 33 h (EPU2), entry minus 15 h (EPU3), and entry minus 6 h (EPU4).

Prelaunch analysis, exemplified in Fig. 11, showed that, under no-margin assumptions, TCM-4 would be the last maneuver needed to fulfill delivery requirements. TCM-5 would not always need to be performed under baseline assumptions, and TCM-6 was just a contingency opportunity to correct gross navigation or planetary ephemeris errors. The analysis also showed that knowledge requirements could be fulfilled in most cases, including that of a launch to Gale on November 26, with a parameter update as early as EPU2. Baseline results were used to generate the entry state dispersions used in EDL Monte Carlo analysis. Those dispersions in delivery and knowledge assumed the execution of TCM-5, with the associated execution errors, and an EPU4 parameter update.

Once the spacecraft was launched, the navigation team started using baseline assumptions to model the uncertainty of the factors affecting the navigation solution. As maneuvers were executed and the solar and thermal radiation pressure model for the spacecraft was

estimated and refined, the uncertainty assumptions were tightened to reflect what was actually observed in the spacecraft. Table 3 lists the different error sources contributing to the orbit determination and prediction accuracy, including how they were modeled during prelaunch analysis and during final approach operations. The values used for MER are also listed for comparison. The following sections describe the different factors affecting the navigation solutions and how the assumptions changed during operations.

A. Measurement Weighting and Range Biases

Range and Doppler measurement weights and range bias uncertainties were assigned based on the performance seen on previous missions and the actual tracking performance observed for MSL. The contribution of changes in the range and Doppler values, in any case, had a very small effect on the combined navigation accuracy. The accuracy was dominated by the plane-of-sky uncertainty, which is better resolved with delta differential oneway range data. The range and Doppler data were weighted by pass, scaling the Doppler postfit residual root mean square (rms) to take into account solar plasma noise effects.

The navigation team used the Δ DOR measurement weights recommended by the Δ DOR team for each observing session, down to 60 ps for a successful three-data-point session. The postfit Δ DOR residual rms was about 38 ps, with the mean residual for some sessions sometimes above this value; see Fig. 12 for an example during approach. Based on the observed navigation performance, it seems that the level of Δ DOR weighting was correct. A tighter weight would have made the solution move in order to fit mean Δ DOR error, and a looser weight would have resulted in bigger predicted uncertainty.

B. Quasars

The position uncertainty of all the quasars used for referencing in differential oneway ranging was assumed to be the same: 1 nrad in right ascension and declination. This value, while a significant improvement with respect to what was used for MER, may have been a conservative estimate of the quasar position error, but it was used in order to protect against possible changes in quasar positions that have occasionally been observed in the past. The actual quasars that were used were carefully selected and did not suffer any position shift, so their position errors were probably much smaller, perhaps on the order of 0.5 nrad. In addition, the same quasar catalog that was used for MSL navigation was also used for the determination of the Mars ephemeris. Over the course of the several years of Δ DOR tracking

Case	1125-0806-M	1125-0806-G	1125-0806-H
Launch Date	25-NOV-2011	25-NOV-2011	25-NOV-2011
Arrival Date	06-AUG-2012	06-AUG-2012	06-AUG-2012
Landing Site Name	Mawrth Vallis	Gale Crater	Holden Crater Fan
Epoch of the Data Arc	E-44.9 days	E-45.5 days	E-45.0 days
Entry Flight Path Angle	- 15.50 deg 0.2 deg	- 15.50 deg 0.2 deg	- 15.50 deg 0.2 deg
Entry Position Knowledge Requirement (3 σ)	2.8 km	2.8 km	2.8 km
Entry Velocity Knowledge Requirement (3 σ)	2.0 m/sec	2.0 m/sec	2.0 m/sec
B-plane Angle	- 26.25 deg	3.96 deg	27.20 deg
dB/d(EFPA)	27.9 km/deg	27.9 km/deg	27.9 km/deg
	Baseline	No-Margin	Baseline
TCM-4 Delivery:			
Data Cutoff Epoch	E-8.4 days	E-8.4 days	E-9.0 days
Apriori TCM-4 Execution Error (3 σ)	7.68 mm/sec	5.92 mm/sec	6.12 mm/sec
Semi-major Axis (3 σ)	6.66 km	4.48 km	7.19 km
Semi-minor Axis (3 σ)	6.12 km	4.34 km	6.62 km
Ellipse Orientation Angle	159.4 deg	156.7 deg	161.6 deg
Linearized Flight Time (3 σ)	1.62 sec	1.14 sec	1.75 sec
Entry Time (3 σ)	4.17 sec	2.87 sec	4.51 sec
B Magnitude (3 σ)	6.66 km	4.48 km	7.11 km
d(3 σ_{EFPA})/d(EFPA)	0.015 deg/deg	0.010 deg/deg	0.016 deg/deg
Entry Flight Path Angle (3 σ)	± 0.24 deg	± 0.16 deg	± 0.25 deg
	± 0.24 deg	± 0.16 deg	± 0.25 deg
TCM-5 Delivery:			
Data Cutoff Epoch	E-2.5 days	E-2.5 days	E-2.5 days
Apriori TCM-5 Execution Error (3 σ)	5.74 mm/sec	3.00 mm/sec	5.76 mm/sec
Semi-major Axis (3 σ)	2.97 km	1.79 km	3.10 km
Semi-minor Axis (3 σ)	2.20 km	1.35 km	2.27 km
Ellipse Orientation Angle	149.4 deg	137.3 deg	149.0 deg
Linearized Flight Time (3 σ)	0.49 sec	0.29 sec	0.50 sec
Entry Time (3 σ)	1.51 sec	0.86 sec	1.51 sec
B Magnitude (3 σ)	2.97 km	1.76 km	2.86 km
d(3 σ_{EFPA})/d(EFPA)	0.007 deg/deg	0.004 deg/deg	0.006 deg/deg
Entry Flight Path Angle (3 σ)	± 0.11 deg	± 0.06 deg	± 0.10 deg
	± 0.11 deg	± 0.06 deg	± 0.06 deg
Entry Knowledge Without TCM-5 (3 σ)			
Position @ E-33h	2.32 km	1.44 km	2.63 km
Velocity @ E-33h	1.32 m/sec	0.82 m/sec	1.56 m/sec
Position @ E-6h	1.16 km	0.81 km	1.58 km
Velocity @ E-6h	0.78 m/sec	0.54 m/sec	1.08 m/sec
Entry Knowledge With TCM-5 (3 σ)			
Position @ E-33h	2.49 km	1.54 km	2.82 km
Velocity @ E-33h	1.41 m/sec	0.88 m/sec	1.68 m/sec
Position @ E-6h	1.24 km	0.84 km	1.67 km
Velocity @ E-6h	0.83 m/sec	0.56 m/sec	1.14 m/sec

Fig. 11 Prelaunch navigation analysis example.

performed in support of Mars ephemeris estimation, a number of the same quasars had been used that were also used for MSL trajectory estimation. This produced a correlation between the quasar errors and ephemeris errors that was not modeled in the MSL navigation filter. This correlation would have had the effect of reducing the error of the MSL trajectory relative to Mars, since a possible quasar position error would have shifted both trajectories in a similar way.

C. Media

The MSL prelaunch analysis and the operational setup for MER both estimated troposphere and ionosphere calibration corrections as stochastic parameters during the DSN tracking sessions. These estimates, while reducing the size of the postfit residuals, did not estimate meaningful media corrections; instead, they just reduced the mean measurement noise of the period of the stochastic batch. The MSL navigation advisory group recommended considering these effects instead. When that change was implemented in the MSL navigation setup, the same a priori uncertainties used to estimate the media parameters stochastically were used to consider them. A smaller uncertainty should have been used since the considered effect was equivalent to a constant error over the filtering arc, whereas the mean effect of a stochastically varying error would be smaller than the uncertainty of a single batch. Also, in this case, since the same system and models that were used for the generation of media calibration for spacecraft navigation were also used for the determination of station and quasar locations and planetary ephemeris, there was a correlation effect that was not taken into account. In addition, while the MSL mission was launched close to the peak of the solar cycle, it was a fairly mild peak; and solar activity, after peaking out during early cruise, remained low during the final approach.

Taking into account all these effects, a more realistic estimate of the mean tropospheric error, when considered, was probably a quarter of what was used during operations, and it was about half in the case of the ionospheric error used during operations.

D. Maneuver Execution Results

The TCMs executed before TCM-4 had ΔV components with sizes between 27.7 mm/s and 5.61 m/s. Execution errors for previous maneuvers had been estimated up to a maximum of 2.3% in magnitude and 2.4 deg in pointing. The largest pointing error occurred for TCM-3, which was the smallest maneuver. TCM-4 was expected to be an even smaller maneuver, so the fixed maneuver execution errors would dominate the total execution uncertainty. TCM-4 had a magnitude error of -5.7%, which was larger than the 3-sigma of the proportional error assumption. However, the maneuver ΔV magnitude was just 11 mm/s and the observed error was small when compared with the fixed error assumption. This relatively good TCM-4 performance meant that no further maneuvers needed to be executed and the remaining maneuvers on approach were canceled. Based on the observed TCM execution performance, it appears that the fixed error assumption may have been conservative, but the postmaneuver orbit determination solution, once $\Delta DORs$ from both baselines were collected, was fairly insensitive to loose TCM execution assumptions. The orbit determination solution would not have performed so well if tighter maneuver execution assumptions had been used.

Postlanding navigation analysis showed that the maneuver execution errors were commensurate with the orbit prediction errors. For each maneuver, the error in achieving the desired target due to the execution error was similar in magnitude to the error due to the trajectory modeling prediction uncertainty.

E. ACS/Navigation Calibration and Turn ΔV Analysis

The thruster combinations used for spacecraft spin rate and spin axis orientation changes were balanced by design, but small errors in thruster alignment or performance could produce a net change in translational velocity. Prelaunch analysis was based on the guidance, navigation, and control requirements and the performance observed

Table 3 Orbit determination assumptions, 1-sigma

Error source	MER final approach operations	MSL prelaunch baseline	MSL prelaunch no-margin	MSL final approach operations	Comments
Two-way Doppler measurement weight	Weight by pass $\geq 0.05 \text{ mm/s}$	0.1 mm/s	0.05 mm/s	Weight by pass $\geq 0.044 \text{ mm/s}$	After removing the spin signature, $3.36 \times \text{rms (60 s) of residuals}$
Range measurement weight	Weight by pass $\geq 0.14 \text{ m}$	3 m	3 m	Weight by pass $\geq 1 \text{ m}$	Per pass/per station
Range biases	2 m/-estimated	2 m/-estimated	1 m/-estimated	1/2 m estimated	Equivalent per session
ΔDOR measurement weight	60 ps	60 ps	40 ps	35 ps	
Station locations errors	Full 2003 covariance considered	Full 2003 covariance considered	Full 2003 covariance considered	Full 2003 covariance considered	
Quasar location errors	2 mrad considered	1 mrad considered	1 mrad considered	1 mrad considered	
Pole X, Y errors	1–4 cm estimated as stochastic	1–4 cm estimated as stochastic	1 cm estimated as stochastic	1 cm considered	
UT1 errors	1.7–9 cm estimated as stochastic	1.7–15 cm estimated as stochastic	1.7–7.5 cm estimated as stochastic	1.7 cm considered	
Ionosphere day/night calibration errors	6.1/1.7 cm estimated as stochastic	6.1/1.7 cm estimated as stochastic	6.1/1.7 cm estimated as stochastic	6.1/1.7 cm considered	
Troposphere wet/dry calibration errors	8/169/294 m considered	1/1 cm estimated as stochastic	1/1 cm estimated as stochastic	1/1 cm considered	
Mars–Earth Ephemeris errors	0.05–0.1 mm/s estimated	0.1 mm/s estimated	0.1 mm/s estimated	13/90/156 m considered	
Turn residual translational ΔV	1.67% estimated	1.67% + 1.33 mm/s Estimated	1.67% + 0.67 mm/s estimated	0.03 mm/s estimated	
Late TCM execution errors	10/10% estimated as bias and stochastic	5/1% estimated as bias and stochastic	2/1% estimated as bias and stochastic	1.67% + 1.33 mm/s estimated	
Solar radiation pressure model errors				2/1% estimated as bias	Specular/diffuse coefficients for MER, in-plane/out-of-plane for MSL

during the MER ACS/NAV calibration and their turn ΔV estimates. A significant effort was made during development to devise an ACS/NAV calibration schema that would provide the most accurate turn ΔV estimates [11]. A kinematic spin removal strategy was implemented to model and remove rotation and nutation effects in order to use the full accuracy of the data, even right after propulsive events [12]. The frame for the ΔV estimation and modeling was also carefully selected to get the most repeatable results.

Actual flight results for the ACS/NAV calibration were better than those used during MER operations and allowed for the use of an uncertainty smaller than that used for prelaunch no-margin analysis. This performance was confirmed during subsequent turns and significantly reduced the effect of turn ΔV uncertainty on the overall navigation performance.

F. Solar and Thermal Radiation Pressure

One of the biggest uncertainties affecting navigation performance was the solar and thermal radiation pressure effects on the trajectory. The Mars Science Laboratory had multiple types of surfaces exposed to the sun: solar panels, the launch adaptor, the parachute cone, antennas, radiators, and sensors. Some of these surfaces were shadowed by each other as a function of the location of the sun with respect to the spin axis of the spacecraft. Surface reflective properties were obtained for the main elements of the spacecraft, and a thermal analysis was made to understand the mean temperature of each element, but this also varied with the changing sun angle and distance to the sun, as shown in Fig. 3. A conscious decision was made not to try to estimate the individual surface properties, as it had been done in most of previous interplanetary missions, but to estimate the overall acceleration as a function of the solar angle. Since the spacecraft was spinning, only the average effect over one or multiple spin periods was important.

A prelaunch radiation pressure model was obtained based on surface properties and thermal analysis, but it was used just to estimate initial values for coefficients of a truncated Fourier expansion on the solar angle. A significant difference with respect to the MER mission was that MSL carried a radioisotope thermal generator that produced a stable level of heat throughout cruise. This, and the fact that the temperatures of the different components changed with the distance to the sun, required adding an empirical stochastic acceleration term along the spin axis that was not modulated with the distance to the sun [11]. During operations, the navigation team estimated the radiation pressure parameters based on tracking data. The set of coefficients that were estimated changed during cruise. By the time of final approach, only a very small set was used that produced excellent trajectory prediction performance.

G. Planetary Ephemeris Updates

Prelaunch analysis used a predicted planetary ephemeris uncertainty that assumed monthly range and ΔDOR tracking of Mars orbiting spacecraft up to three months before entry. Two planetary ephemeris sets were generated specifically for the MSL project: DE424, generated two months before launch; and DE425, generated three months before entry. The change between the two, since they shared most of the data used to create them, was just tens of meters, which was much smaller than the uncertainty estimated at entry. These ephemerides benefited from ΔDOR tracking of the Mars orbiters for more than two Earth–Mars synodic periods.

As mentioned before, the Mars–Earth ephemeris uncertainty estimated for DE425 and used by MSL did not take into account the effect of using some error sources that were common to both the planetary and spacecraft ephemerides, such as the quasar and DSN station coordinates or media calibration models. That made the navigation uncertainty estimate somewhat conservative.

H. Final Approach Results

Once the radiation pressure model had been simplified and improved using the estimates obtained during midcruise, the late-cruise trajectory prediction performance was excellent. Figure 4 shows the range data residuals that were obtained when processing three weeks

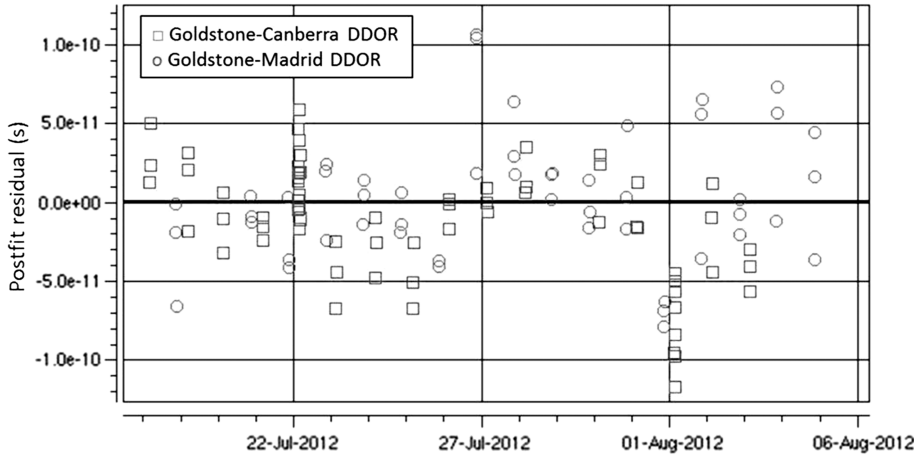
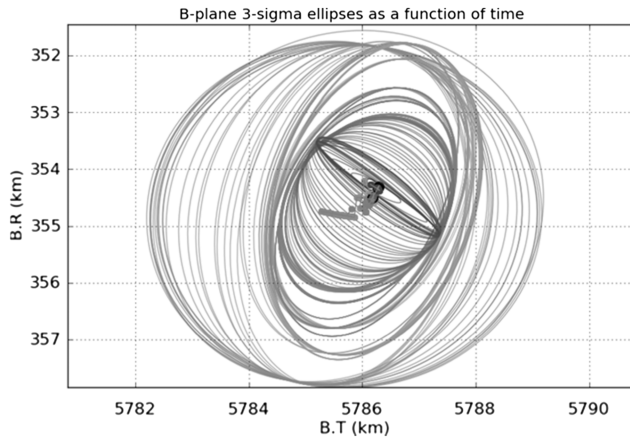
Fig. 12 ΔDOR postfit residuals for the final approach.

Fig. 13 Evolution of the trajectory solution and 3-sigma uncertainty from TCM-4 execution to entry. The ellipse size decreases as time increases.

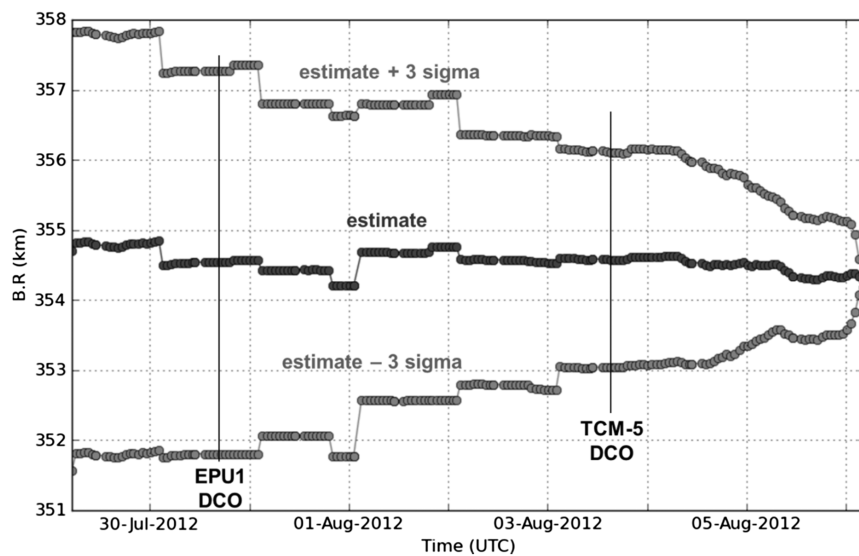
of data, ending before TCM-4, and using a solution obtained one week after TCM-3. The data displayed were not used in the solution, as it was received after the data cutoff. This meant that the line-of-sight position of the spacecraft was predicted to better than 10 m over three weeks of prediction: a remarkable feat anywhere in the solar system. This performance could be obtained even in the presence of two turns, indicating that the turn ΔV estimates were also very precise. This kind of performance gave us a high confidence that, in

absence of unexpected events or gross TCM-4 execution errors, the trajectory estimates should be very stable.

Figure 13 shows the evolution of the trajectory solution in the B plane after TCM-4 as a function of the data cutoff, using all the best available calibrations, and at steps of 1 h. The operational solutions, as shown in Fig. 8, evolved in a similar way. The dots represent the best estimate of the solution, whereas the ellipses represent the 3-sigma uncertainty level associated with each solution. It is evident that the variation seen in the solution estimates is considerably smaller than what should be expected based on the associated uncertainties.

Figures 14 and 15 show the evolution of the two B-plane coordinates, as well as the data cutoffs for the first entry parameter generation, EPU1, and for the TCM-5 maneuver opportunity. Changes in $B \cdot T$ were mostly aligned with changes in entry flight-path angle and longitude, whereas changes in $B \cdot R$ represented mostly changes in entry latitude.

The effect of adding ΔDOR sessions to the solution is more obvious in Fig. 14, as they simultaneously make the best estimate of $B \cdot R$ jump and its uncertainty decrease. The effect of the errors and uncertainty of the planetary ephemeris can be seen in the last 48 h of the estimates, when the uncertainties contract, first gradually and then rapidly for the last hours, as Doppler becomes more sensitive to the Mars position. The initial uncertainty level was dominated by the TCM-4 maneuver execution uncertainty. However, since the TCM-4 execution was fairly accurate, the uncertainty decreased as more tracking data were added without significantly changing the actual estimates.

Fig. 14 Evolution of the B-plane $B \cdot R$ coordinate estimate during the final approach.

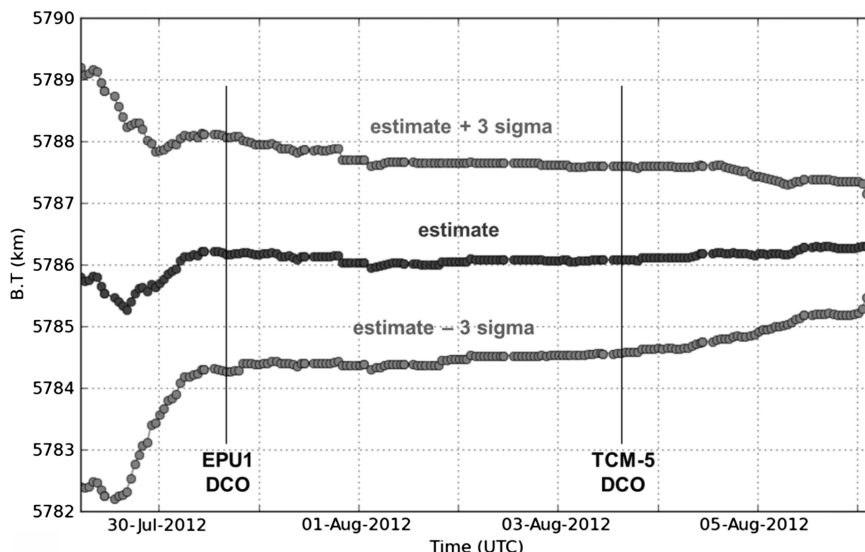


Fig. 15 Evolution of the B-plane $B \cdot T$ coordinate estimate during the final approach.

The relatively accurate execution of TCM-4 and the excellent trajectory prediction performance allowed for the cancellation of the TCM-5 and TCM-6 maneuvers, as well as the cancellation of the EPU2, EPU3, and EPU4 entry parameter updates. When the EPUs for the data cutoffs at entry minus 33, 14, and 6 h were evaluated, the orbit solutions had not moved significantly, either in the B plane or when propagated to the ground using EPU1. This fed into the decision to cancel all planned updates of the onboard state. By the time of the last update, the line-of-sight residuals with respect to the EPU1 solution were just 2 m off.

Postlanding analysis, using all the data up to entry and the final calibrations, showed that the actual entry state differed from the EPU1 state onboard the spacecraft by just 200 m in position and 0.11 m/s in velocity. Additionally the entry flight-path angle was just 0.013 deg shallower than the -15.5 deg requirement.

I. Reassessment of the Final Approach Covariance

The evolution of the solutions between the execution of TCM-4 and the TCM-5 DCOs could be divided into two segments: the first segment of about three days in which the TCM-4 maneuver execution error is being resolved, and the orbit uncertainty decreasing steadily; and a second segment of about 2.5 days with fairly constant orbit uncertainty.

For the first segment, the initial covariance was dominated by the maneuver execution uncertainty. Operational experience before TCM-4 seemed to indicate that the actual maneuver execution performance was somewhat better than the prelaunch requirements. But since the magnitude of the maneuvers executed so far was larger than that planned for TCM-4, it was not possible to determine whether the proportional errors or the fixed errors were dominant. The navigation team generated solution uncertainties based on different TCM-4 maneuver execution error levels; it was clear that TCM-5 would not be needed if TCM-4 was executed with accuracy proportional to that seen for previous maneuvers. The line-of-sight error observed during the execution of TCM-4 was larger than that observed for previous maneuvers, so there was no compelling reason to reduce the TCM-4 maneuver uncertainty assumptions after it was executed. As a matter of fact, later analysis showed that, if we had used a smaller maneuver execution uncertainty in combination with limited data after maneuver execution, the solution would have moved more and we would have had a worse entry state estimate for EPU1. EPU1 was generated using just one Δ DOR session from each of the DSN baselines, but those data, combined with a not-too-constrained TCM-4, were enough to fairly accurately determine TCM-4. This, together with the good trajectory prediction performance using the final radiation pressure model, produced an entry state estimate that was very close to truth.

For the second segment, the uncertainty of the trajectory solution up to the TCM-5 DCO seemed bigger than what it should have been, when one compares the uncertainty to the changes in the trajectory estimate up to entry. There is always the possibility of dumb luck but, given the consistency of the solution between EPU1 and entry, it seemed to be more than just luck that we got the solution right at EPU1. Some of our uncertainty assumptions were probably too conservative, and a more realistic estimate of the solution uncertainty should have been smaller.

There were other indications during cruise that our navigation performance was better than what our covariance analysis indicated. One was the performance of range residual using predicted trajectories, as shown previously in Fig. 4. Another was the evaluation of tracking data residuals for the Mars orbiters, as shown in Figs. 5–6. The range residuals obtained were below 10 m, whereas mean residuals for Δ DOR sessions were in the 200 m level for the plane-of-sky position coordinates. Phase referencing interferometry sessions were also performed between MSL and MRO; the residuals for those (Fig. 7) were also at the same 200 m level.

As described in previous sections, postlanding scrubbing of the covariance assumptions found some candidates for the conservatism observed in the navigation uncertainty estimates. Media uncertainties were too conservative when the errors were being considered because the effect was the same as assuming a constant error. Ionospheric calibration errors were not as big as expected, even at the top of the solar cycle, since this was a fairly mild cycle and the sun was not very active during the final approach. Quasar position uncertainties were at an appropriate level when the choice of the particular quasars to be used was not known, and to protect against quasar position shifts observed in some quasars; however, in hindsight, they were conservative given the performance of the actual quasars that were used during operations. In addition, while we used absolute error estimates for each of our error sources, those estimates included the errors from some of the same sources that we were modeling. Quasar and DSN station coordinate errors affected both the planetary ephemeris solution and the MSL trajectory solution, but the resulting ephemeris errors may have been correlated, thereby reducing the error of MSL relative to Mars.

VIII. Conclusions

The Mars Science Laboratory navigation team, and the other teams supporting it, accurately navigated the spacecraft to Mars, possibly at the limit of what is possible with current calibration and tracking measurement errors. The main contributors to this excellent performance were the hard work and dedication of everybody involved, the high accuracy of the Deep Space Network radiometric and calibration data, the careful modeling of the spacecraft attitude and its

radiation pressure forces, and the conscious choice to optimize the navigation filter in order to improve the trajectory prediction performance by drastically reducing the set of parameters being estimated and by properly weighting the tracking measurements, without trying to overfit noisy data.

Looking back at the navigation error assumptions used during development and operations, the only clearly conservative assumptions that were used were the tropospheric calibration uncertainties and neglecting the correlation between planetary ephemeris and quasar and tracking station coordinate errors. But changing these assumptions would not have made a significant difference when comparing the operational results with the no-margin results. During operations, the B-plane uncertainties were still dominated by maneuver execution error assumptions. Without a dedicated calibration campaign for small trajectory correction maneuvers, operationally time-consuming and risky, it may not have been possible to reduce those assumptions. Maneuver execution performance was adequate early in the mission since the effect of maneuver execution errors was comparable to the effect of trajectory prediction errors. More accurate execution would only have made a difference for planning maneuver and parameter update opportunities during final approach. In addition, landing ellipse size was also not dominated by interplanetary navigation errors but by attitude initialization and Mars atmosphere mismodeling errors. Nevertheless, the excellent interplanetary navigation performance made it possible to free up time during the final approach for other more pressing activities, and it helped to ensure a successful entry, descent, and landing, and an accurate delivery to the desired landing target inside Gale Crater.

Acknowledgments

This research was carried out at the Jet Propulsion Laboratory, California Institute of Technology (JPL), under a contract with NASA. The authors would like to acknowledge the contribution to the rest of the Mars Science Laboratory (MSL) navigation team: E. D. Gustafson, N. A. Mottinger, J. S. Border, C. A. Halsell, T. P. McElrath, F. Pelletier, P. F. Thompson, C. G. Ballard, J. Casoliva, M. S. Ryne, and D. C. Jefferson. The excellent MSL navigation performance presented in this paper was the result of not only the efforts of the entire navigation team but also of a number of people that provided excellent support to the team, including Jae Lee (Systems Administrator) and Vic Legerton (Navigation Ground Data System Engineer). Our special thanks to Bill Folkner, from the JPL's Solar System Dynamics Group, who created the very precise Mars ephemeris used by MSL; and to Lou D'Amario, who led the MSL Mission Design and Navigation Team during the development phase. We also want to recognize the help from the Navigation Advisory Group, led by Joe Guinn, and the excellent support from the Deep Space Network and JPL's Tracking Systems and Applications section. Reference herein to any specific commercial product, process, or service by trade name, trademark, manufacturer, or otherwise, does not constitute or imply its endorsement by the U.S. Government or the Jet Propulsion Laboratory, California Institute of Technology.

References

- [1] Grotzinger, J., Crisp, J., Vasavada, A. R., Anderson, R. C., Baker, C. J., Barry, R., Blake, D. F., Conrad, P., Edgett, K. S., and Ferdowski, B., et al., "Mars Science Laboratory Mission and Science Investigation," *Space Science Reviews*, Vol. 170, Nos. 1–4, 2012, pp. 5–56.
doi:10.1007/s11214-012-9892-2
- [2] Steltzner, A., "Mars Science Laboratory Entry, Descent and Landing System Overview," *AAS/AIAA Space Flight Mechanics Meeting*, American Astronomical Soc. Paper AAS-13-236, 2012.
- [3] Golombek, M., Grant, J., Kipp, D., Vasavada, A., Kirk, R., Ferguson, R., Bellutta, P., Calef, F., Larsen, K., and Katayama, Y., et al., "Selection of the Mars Science Laboratory Landing Site," *Space Science Reviews*, Vol. 170, Nos. 1–4, 2012, pp. 641–737.
doi:10.1007/s11214-012-9916-y
- [4] D'Amario, L. A., "Mars Exploration Rovers Navigation Results," *AIAA/AAS Astrodynamics Specialist Conference*, AIAA Paper 2004-4980, 2004.
- [5] Abilleira, F., "2011 Mars Science Laboratory Launch Period Design," *AAS/AIAA Astrodynamics Specialist Conference*, American Astronomical Soc. Paper AAS-11-553, 2011.
- [6] D'Amario, L. A., "Mission and Navigation Design for the 2009 Mars Science Laboratory Mission," *59th International Astronautical Congress*, Paper IAC-08-A.3.3.A1, 2008.
- [7] Makovsky, A., Ilott, P., and Taylor, J., "Mars Science Laboratory Telecommunications System Design," *DESCANSO Design and Performance Summary Series*, Jet Propulsion Lab., California Inst. of Technology Article 14, Pasadena, CA, 2009.
- [8] Wong, M. C., Kangas, J. A., Ballard, C. G., Gustafson, E. D., and Martin-Mur, T. J., "Mars Science Laboratory Propulsive Maneuver Design and Execution," *23rd International Symposium on Space Flight Dynamics*, Pasadena, CA, 2012.
- [9] Thornton, C. L., and Border, J. S., "Radiometric Tracking Techniques for Deep-Space Navigation," Monograph 1, Deep-Space Communications and Navigation Series, Jet Propulsion Lab., California Inst. of Technology Publ. 00-1-1, Pasadena, CA, Oct. 2000.
- [10] Folkner, W. M., "Planetary Ephemeris DE424 for Mars Science Laboratory Early Cruise Navigation," Jet Propulsion Lab., California Inst. of Technology Interoffice Memo. IOM-343R-11-003, Pasadena, CA, Sept. 2011.
- [11] Kruizinga, G. L., Gustafson, E. D., Thompson, P. F., Jefferson, D. C., Martin-Mur, T. J., Mottinger, N. A., Pelletier, F. J., and Ryne, M. S., "Mars Science Laboratory Orbit Determination," *23rd International Symposium on Space Flight Dynamics*, Pasadena, CA, 2012.
- [12] Gustafson, E. D., Kruizinga, G. L., and Martin-Mur, T. J., "Mars Science Laboratory Orbit Determination Data Pre-Processing," *AAS/AIAA Space Flight Mechanics Meeting*, American Astronomical Soc. Paper AAS-13-231, 2012.
- [13] Thompson, P. F., Gustafson, E. D., Kruizinga, G. L., and Martin-Mur, T. J., "Filter Strategies for Mars Science Laboratory Orbit Determination," *AAS/AIAA Space Flight Mechanics Meeting*, American Astronomical Soc. Paper AAS-13-233, 2012.
- [14] Chen, A., Greco, M., Martin-Mur, T., Portock, B., and Steltzner, A., "Approach and Entry Descent, and Landing Operations for the Mars Science Laboratory Mission," *AAS/AIAA Space Flight Mechanics Meeting*, American Astronomical Soc. Paper AAS-13-425, 2012.
- [15] Burkhardt, P. D., and Casoliva, J., "MSL DSENDs EDL Analysis and Operations," *23rd International Symposium on Space Flight Dynamics*, Pasadena, CA, 2012.
- [16] Abilleira, F., and Shidner, J. D., "Entry, Descent, and Landing Communications for the 2011 Mars Science Laboratory," *23rd International Symposium on Space Flight Dynamics*, Pasadena, CA, 2012.
- [17] Abilleira, F., "2011 Mars Science Laboratory Trajectory Reconstruction and Performance from Launch Through Landing," *AAS/AIAA Space Flight Mechanics Meeting*, American Astronomical Soc. Paper AAS-13-234, 2012.
- [18] Sergeyevsky, A. B., Snyder, G. C., and Cinniff, R. A., "Interplanetary Mission Design Handbook," Jet Propulsion Lab., California Inst. of Technology Publ. 82-43, Pasadena, CA, 15 Sept. 1983.
- [19] Martin-Mur, T. J., Kruizinga, G. L., and Wong, M., "Mars Science Laboratory Interplanetary Navigation Analysis," *22nd International Symposium on Space Flight Dynamics*, Sao Jose dos Campos, Brazil, 2011.

R. Braun
Associate Editor